24th International Conference on Renewable Energies and Power Quality (ICREPQ'26)
Santander (Spain), 10th to 12th June 2026
ISBN-13: 978-84-09-82044-3

Evaluation of Fixed-Tilt and Single-Axis Tracking Strategies in Open-Field Agrivoltaics: Assessing Biological Constraints and Economic Viability

A. León-Vinet[1], E. Peñalvo-López[1], I. Valencia-Salazar[1] and V. León-Martínez[1]

[1] Universitat Politècnica de València, Department of Electrical Engineering
Camí de Vera, s/n, 46022 València (Spain)

e-mail: amleovi@etsii.upv.es, elpealpe@upvnet.upv.es, ivalencias@die.upv.es, vleon@die.upv.es

Abstract. This study evaluates the performance of an agrivoltaic system located in Valencia (Spain) over a 6-month period (mid-March to mid-September) by analysing the interaction between photovoltaic (PV) generation, water consumption, and the physiological requirements of the crop, in this case *Citrus limon* (lemon). The research compares fixed-tilt panels against single-axis trackers. For the tracking system, two algorithms were modelled: pure energy maximisation, and a yield-constrained model.

While the model is based on empirically validated equations, the results represent simulated potential and have not yet been field-validated. Results indicate significant variations relative to a conventional farm. The yield-constrained single-axis model decreased crop yield by 24.84% and reduced water consumption by 4.02%, achieving a total economic benefit of 6,437.29 €. The energy-maximisation single-axis model resulted in a decrease in yield (26.75%) and water consumption (4.95%), generating an income benefit of 6,676.08 €. The fixed-tilt system provided the highest economic return for the period (6,808.03 €), with yield and water consumption decreasing by 25.04% and 4.10%, respectively.

Regarding energy production relative to the fixed-tilt baseline, the energy-maximisation tracker achieved a 9.14% increase, whereas the yield-constrained tracker resulted in a 7.14% increase. These findings suggest that while agrivoltaics reduce overall crop yield due to shading in Mediterranean climates, their energy generation heavily compensates for agricultural deficits, ensuring strong economic viability despite biological and market sensitivities.

Key words. Agrivoltaics, energy, agriculture, electricity, solar panel.

1. Introduction

Food and energy security are deeply interlinked [1], as the current global energy crisis [2] [3] and the climate emergency necessitate a 42% reduction in greenhouse gases to reach the 1.5°C by 2030 [4]. The agricultural sector, responsible for over 10% of Europe's greenhouse gas emissions in 2022 [5], is highly sensitive to energy consumption [6] [7]. Agrivoltaics is the dual use of the land for solar energy and farming [8], offers a sustainable solution to increase land yield, and is currently being considered in various European Union countries [9].

While the study and implementation of agrivoltaics have increased in recent years [10], most existing models do not fully consider specific crop requirements or current legislation. Research typically focuses on static design parameters [11] (such as height, row spacing, and orientation) and general crop behaviour [12]. There is a lack of focus on the hourly optimization of adjustable solar panel variables to ensure the specific needs of each plant are met, as well as the subsequent effects on the farm's overall water and energy consumption.

2. Objective

This paper presents a novel methodology for evaluating the crop parameters, including PV energy generation,

the modelled behaviour of a 1-axis agrivoltaic system, focusing on the maximisation of electrical energy generation while satisfying the physiological needs and biological constraints of the underlying crops. The study aims to evaluate how these operational changes affect the overall energy and water consumption of the farm.

The crop specimens used for the simulation are adult *citrus limon*, commonly known as lemon trees.

3. Parameters

The maximisation methodology considers the following:

A. Location and Time Range

The geographical coordinates of the site are essential to accurately model solar positioning and irradiance. The simulation is set in Valencia, Spain. The temporal scope covers the six warmest months of 2021 to capture peak thermal stress and irrigation demand.

Table I. – Time range, latitude, longitude, altitude

	VALUE
Time range	[15/03/2021, 01:00] – [16/09/2021, 00:00]
Latitude	39.47391
Longitude	-0.37966
Altitude	150

B. *Dimensions of agrivoltaic farm*

The base agrivoltaic system comprises 176 solar panels covering a 2,678.5 m^2 area. This plot contains 89 lemon trees with canopy dimensions of 3x3 m and a spacing of 5x7 m. To ensure rigorous comparison, the baseline scenario consists of a conventional *Lemon citrus* farm with the same dimensions, plant density, and location, but without the presence of photovoltaic structures.

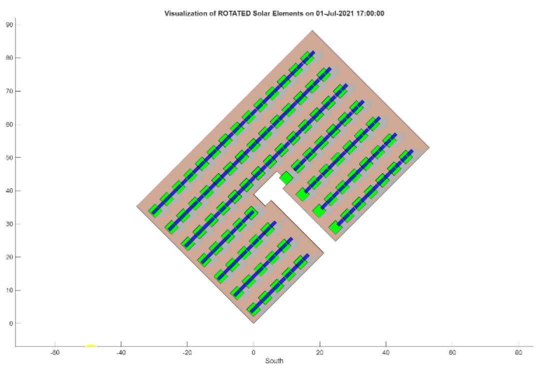

Fig. 1. Visualisation of the agrivoltaic farm

C. *Solar Plant and Panel Typology*

Panel typology determines both solar irradiance and the physical-mechanical behaviour of the system. Following the trans-disciplinary approach of Toledo et al. [13], this study distinguishes between agrivoltaic patterns and photovoltaic greenhouses. The analysis focuses on orientation (azimuth and tilt) and system typology, comparing fixed-tilt and 1-axis tracking configurations.

CAPEX and OPEX values of the solar plant (Table II) are based on average 2021 industry estimates for elevated agrivoltaic structures [14] [15].

Table II. - Solar panel characteristics (source: own elaboration)

	VALUE	UNITS
Size X axis	2.27	m
Size Y axis	1.13	m
Size Z axis	0.05	m
Height	4.00	m
Capacity PV array	600	W
Derating factor	0.85	%
Radiation test	1000	W / m^2
Temperature Coeff.	-0.0049	% / °C
Temperature Standard	25	°C
Installation cost, fixed	1,200.00	€ / kWp
Installation cost, 1-axis	1,500.00	€ / kWp
Maintenance cost, fixed	25.00	€ / kWp
Maintenance cost, 1-axis	35.00	€ / kWp
Lifespan	20	years

D. *Weather and economic data*

Hourly weather data (rainfall, temperature, GHI, and humidity) has been obtained from Open-meteo [16].

E. *Energy, Water, and Crop Prices*

Electric pricing data (purchase and sale) were obtained from the e-sios platform [17], for the Spanish market in 2021, reflecting hourly market volatility. Water prices are based on the 2021 Segura-Júcar basin costs of 0.16 € / m^3 [18]. Lemon prices were set at 0.10 € / kg based on 2021-2022 market reports [19].

F. *Crop Typology*

Crops have different needs depending on their type and their growth phase. The biological model simulates the actual biological process of the plant using evapotranspiration (ET) and photosynthetic active radiation (PAR), together with different stress factors to calculate the final yield of the crop. This information is needed to calculate solar and irrigation needs.

Data for lemon trees can be found in FAO databases [20].

Table III. – Crop and soil characteristics for *citrus limon* [20]

FORMULA	VARIABLE	VALUE	UNITS
Evapotranspiration	Crop factor (K_c)	[0.65 – 0.70]	[0 – 1]
	Canopy Cover (CC)	0.80	[0 – 1]
	Maximum evaporation (K_{ex})	0.45	[0 – 1]
	Crop transpiration coefficient (K_{cTr})	[0.52 – 0.56]	[0 – 1]
Harvest Index	Percentage of energy used by the plant for respiration (R_m)	0.45	[0 – 1]
	Partition factor (P_f)	0.65	[0 – 1]
	Percentage of dry matter in the fruit (DM_{conc})	0.15	[0 – 1]
Crop yield	Fraction of light intercepted (f_{int})	0.80	[0 – 1]
	Radiation Use Efficiency (RUE_{max})	1.6	g / MJ

G. *Energy consumption*

This study assumes no additional electrical energy consumption besides the hydraulic pump. Pump data is based on technical specifications provided by Chandel et al. [21]

Table IV. – Pump characteristics (source: [21])

	VALUE	UNITS
Efficiency	60	%
Head height	25	m
Flowrate	5000	L / h
Mode	Interval with wilting point	
Time between pumps	7	days

4. Methodology

The proposed methodology integrates established sub-models into a novel decision-making loop. While sun-position (SPA) [22], evapotranspiration (FAO-56) [23], and panel performance (Sandia/HOMER) [24] [25] are based on validated literature, the methodological novelty lies in the hourly iterative coupling of physiological crop constraints with 1-axis tracker optimization to prioritize biological survival over energy harvesting.

The model consists of a loop that iterates hourly during the established period. These loops include calculations for the agrivoltaic system and for a non-agrivoltaic farm. The steps within the loop are detailed below.

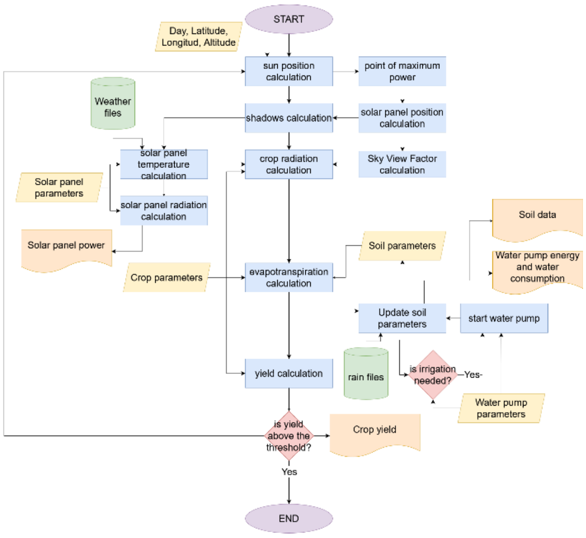

Fig. 2. Methodology diagram for each iteration

A. *Initial solar values and solar panel orientation*

First step before starting the loop is to indicate the coordinates and dimensions for the crops and the solar panels. Crops must be positioned individually to understand the shadow effects on them. The orientation of the cropland is crucial to proceed adequately with future calculations.

Calculations are performed at hourly time steps, consistent with FAO Penman-Monteith requirements [23].

The sun position is obtained via NREL's solar position algorithm (SPA) **[22]** based on both timescale and location. Solar panels are assumed to not receive shadows due to a) ensured minimal no-shadow distance between panels and b) panels being at minimum the same height of the crops.

Initial orientation of the solar panels is either calculated internally following the point of maximum power or based on PVGIS optimum inclination [26], depending on the type of solar panel (1-axis or fixed). For tracking configurations, the optimal angle is determined using *fmincon* with a multi-start strategy employing up to five initial points to avoid convergence to local minima, particularly around solar noon when the optimal tracking angle changes sign abruptly.

B. *Solar panel temperature and power output*

Temperature of the solar panel module and cell are calculated using the simplified Sandia National Laboratories model, developed by King et al., [25], with the Faiman parametrisation [27]. To calculate the PV array power output, HOMER equation is used, with temperature effect included **[24]**.

C. *Initial solar values and crop radiation calculation*

Radiation values of each crop are needed for evapotranspiration and yield. Net radiation R_n is the difference between net shortwave radiation (R_{ns}) and net longwave radiation (R_{nl}). Both values calculated using FAO equations [23] depend on the total incident radiation (R_s) obtained from sun position calculations, the shading percentage experienced by each crop, and the Sky View Factor (SVF).

Total incident radiation (R_s) is calculated as:

$$R_s = [S \cdot R_{dir}] + [SVF \cdot R_{dif}] \tag{1}$$

Where:

R_s total incident radiation [MJ m^{-2} hour^{-1}],
S shading percentage experience by the crop each instant [%].
R_{dir} direct radiation on the crop [MJ m^{-2} hour^{-1}],
SVF sky view factor of the crop [%],
R_{diff} diffuse radiation on the crop [MJ m^{-2} hour^{-1}].

The shading percentage experienced by each crop is calculated using computational geometry (MATLAB *polyshape*). Shadows of both the solar panels and their support structures are projected onto the ground plane. The convex hull of each projected shadow is computed and merged into a global shadow *polyshape*, which is then intersected with each crop's projected canopy area to determine the overlap percentage.

The Sky View Factor (SVF) is a dimensionless parameter primarily used in urban climatology that measures the proportion of sky visible from a specific point on the ground [28]. Rather than assuming a homogeneous distribution, the SVF is calculated individually for each crop position using Howell's analytical view factor integration [29]. For each plant-panel pair, the angle of the panel as seen from the plant is computed using the rectangular view factor equation:

$$VF_p = F(x_2, y_2) - F(x_1, y_2) - F(x_2, y_1) + F(x_1, y_1) \tag{2}$$

Where:

$$F(x,y) = \frac{1}{2\pi}\left[\frac{x}{\sqrt{1+x^2}} arctan\left(\frac{y}{\sqrt{1+x^2}}\right) + \frac{y}{\sqrt{1+y^2}} arctan\left(\frac{x}{\sqrt{1+y^2}}\right)\right] \tag{3}$$

And x_1, x_2, y_1, y_2 are the dimensionless coordinates of the panel edges relative to the plant position, scaled by the vertical distance h between the panel and the plant canopy. The total SVF at each plant position is obtained by subtracting the accumulated view factors of all panels:

$$SVF_{matrix} = max\left(0.05, 1 - \sum_{p=1}^{N} VF_p\right) \tag{4}$$

This approach accounts for the actual 3D geometry of each panel (position, height, tilt, and projected dimensions) relative to each individual plant, yielding a spatially resolved SVF matrix rather than a single aggregate value.

D. Crop evapotranspiration for biological model

Evapotranspiration (ET) is the combination of two separate processes by which water is lost from the soil surface through evaporation and crop transpiration [23]. Crops have evapotranspiration needs depending on their type and their growth phase. This value is composed of the multiplication of two different factors: the reference evapotranspiration (ET_o), which is divided into evaporation and transpiration, and the crop factor (K_c).

ET_o value is calculated using FAO Penman-Monteith equation [23] with hourly time steps and updated for day and night changes according to ASCE-EWRI [30].

Both evaporation and transpiration are calculated using AquaCrop model [31].

Final evapotranspiration (ET) is individually calculated for each of the plants in the crop and subtracted from the current soil moisture affecting it.

A microclimate temperature model is included to capture the thermal effect of the panel structures on the near-ground environment. The model computes the microclimate air temperature and canopy temperature at each plant position. For the agrivoltaics scenario, the convective heat released by the heated panel surfaces is included as an additional energy input. These microclimate temperatures feed directly into both the evapotranspiration calculation and the heat stress factor used in the yield model.

E. Water pump function for biological model

Depending on the current humidity of the soil, affected by evapotranspiration and rain, the water pump will activate according to the time interval stated.

Soil moisture is tracked individually for each plant position as a grid, for the agrivoltaic scenario and the baseline. When the soil moisture of any plant in the farm reaches the wilting point, the water pump actives earlier and restarts the interval count. Irrigation affects the entire farm uniformly, as no individual drip irrigation is modelled.

The energy source for the pump is determined hourly: if the current PV generation exceeds the pump's power demand, the energy is self-consumed at zero marginal cost; otherwise, electricity is purchased from the grid at the hourly rate.

F. Crop yield calculation for biological model

Knowing both the photosynthetic radiation received and the evapotranspiration of the crop, hourly yield data is calculated and compared to the baseline. A comparison is then made to the original farmland. Based on DIN SPEC 91434 [32], if the hourly yield is below 66% and the solar panels can be moved, then those will be moved. If the solar panels cannot be moved, it will only take this information into account and inform at the end of the iteration if the threshold has been reached.

Photosynthetic active radiation (PAR) typically accounts for between 44% and 69% of global solar radiation [33]. Current values used are Zhu et al. [34] of 48.7%, which will be used also during the yield calculation.

Environmental conditions can penalise the growth of the crop in the form of heat stress (K_h) and water stress (K_s).

For heat stress, a trapezoidal model based on the acceptable temperature ranges of the plant due its simplicity and high sensibility towards heat stress [35].

For water stress, the model considers the wilting point, which is the soil moisture level at which plants cannot extract water from the soil, and the depletion fraction, at which point plants start suffering the effects of drought.

Crop yield is estimated following Monteith radiation use efficiency approach [36] with AquaCrop structure adjusted by environmental stress indices and the harvest index [31].

G. Minimum yield condition

Based on DIN SPEC 91434 [32], the farm yield must be at least 66% of a non-agrivoltaic system. In this study, a stricter constraint is applied: each individual tree must reach 85% of its potential yield. This constraint is enforced within the *fmincon* optimisation loop as a nonlinear inequality. Yield percentages are calculated as the cumulative biomass production over the 6-month period, individually tracked per plant and then aggregated to the farm level for both constraint evaluation and economic assessment. It should be noted that evapotranspiration is not recalculated within the optimisation sub-routine: the soil moisture state from the previous time step is used as an approximation to reduce computational cost.

5. Results

Three simulations were performed based on solar panel movement restrictions: fixed-tilt, 1-axis without minimum yield, and 1-axis with minimum yield.

Table V. – Results for the 6-month period for all three simulations. (Source: Own elaboration)

	AGRIPV FIXED	AGRIPV ONE AXIS, NO MINIMUM	AGRIPV ONE AXIS, MINIMUM YIELD	BASELINE
PV energy generated (kWh)	143,026.04	156,102.77	153,245.07	0.00
Pump energy consumed (kWh)	174.01	172.45	174.14	181.43
Pumped water (L)	1,532,529.15	1,518,826.16	1,533,709.29	1,597,985.29

Crop yield (kg / m^2)	3.73	3.65	3.75	4.98
Relative crop yield (%)	74.96	73.25	75.16	100.00
Econ. benefit PV energy sold (€)	11,251.86	12,447.41	12,203.36	0.00
Economic benefit crop yield (€)	299.15	292.34	299.98	399.11
PV prorated depreciation (€)	3,174.90	3,968.63	3,968.63	0.00
Solar panel maintenance cost (€)	1,322.88	1,852.03	1,852.03	0.00
Pump energy cost (€)	0.00	0.00	0.00	29.64
Pump water cost (€)	245.20	243.01	245.39	255.68
Total economic benefit (€)	6,808.03	6,676.08	6,437.29	113.79

There is an increase in PV energy generated of 9.14% in the 1-axis model that disregards the minimum yield of the crops and focuses on the maximisation of energy compared to the fixed model, and an increase of 1.86% compared to the yield-constrained 1-axis model.

Regarding crop production, the cumulative relative yield between the different setups varied, with the lowest overall yield being 73.25% (energy-maximizing 1-axis system) and the highest reaching 75.16% (yield-constrained 1-axis system), both remaining below the 100% baseline.

Water consumption decreased across all agrivoltaic setups (between 4.02% and 4.95%), largely due to the reduced temperature (both soil and crops) and the reduced yield in the agrivoltaic models. While the panels mitigate extreme heat stress and excessive evapotranspiration during the Mediterranean summer by providing a protective microclimate, this was not enough to fully compensate for the reduction of Photosynthetic Active Radiation (PAR) caused by the shading, resulting in lower yields across all PV configurations compared to the baseline.

The fixed-axis system offers a superior economic outcome (6,808.03 €) due to the reduced capital and maintenance expenditures, practically matching the total benefit of the energy-maximizing model. The low market price of the crops does not economically justify higher installation costs for the trackers. However, all three agrivoltaic systems are financially viable and highly positive compared to the baseline model, which achieves a total benefit of only 113.79 € for the period due to the low price paid to the farmers for their crops.

6. Conclusions

The presented simulation framework provides a theoretical estimation of yield values, radiation, and humidity requirements at the individual plant level, facilitating the dynamic adjustment of solar panel inclination to meet specific physiological needs. However, it is important to note that these results are derived from numerical simulations and have not yet been empirically validated. While the model indicates a yield decrease these findings should be interpreted as theoretical potentials within the modelled constraints, as the reported gains in crop yield and economic benefit are subject to the uncertainties of the biological sub-models.

Currently, the model relies on fixed initial space coordinates for both panels and crops. Later versions will include the option of placing solar panels in the optimal position based on specific crop physiology and panel typology. Furthermore, the model is designed to evolve into a multi-objective optimisation tool, capable of prioritizing variables such as total economic benefit, crop yield maximisation, or water conservation through independent panel tracking.

This framework provides agricultural stakeholders a strategy for revenue diversification and operational cost reduction, specifically regarding irrigation pumping, without compromising farm's overall financial stability.

Acknowledgement

This work was developed under the Universitat Politècnica de València and the PhD Program in Design, Manufacturing, and Management of Industrial Projects.

References

[1] P. David, L. E. Hurd, A. C. Bellotti, M. J. Forster, I. N. Oka, O. D. Sholes and R. J. Whitman, "Food Production and the Energy Crisis," *Science,* vol. 182, pp. 443-449, 1973.

[2] Organización de las Naciones Unidas, *Agenda 2030 sobre el Desarrollo Sostenible,* 2015.

[3] Comisión Europea, *REPowerEU - Affordable, secure and sustainable energy for Europe,* 2024.

[4] Organización de las Naciones Unidas, *Emissions Gap Report 2023: Broken Record – Temperatures hit new highs, yet world fails to cut emissions (again),* 2023.

[5] Agencia Europea del Medio Ambiente, "Emisiones de gases de efecto invernadero por país y sector (infografía)," 2024. [Online]. Available: https://www.europarl.europa.eu/portal/en.

[6] F. Felloni, T. Wahl and P. Wandschneider, "Evidence of the effect of infrastructure on agricultural production and productivity: implications for China," 1996.

[7] O. Karkacier, Z. G. Goktolga and A. Cicek, "A regression analysis of the effect of energy use in agriculture," *Energy Policy,* vol. 34, no. 18, pp. 3796-3800, 2006.

[8] A. Goetzberger and A. Zastrow, "On the Coexistence of Solar Energy Conversion and Plant Cultivation," *International Journal of Solar Energy, 1,* pp. 55-69, 1982.

[9] Comisión Europea, "Common Agricultural Policy," 2020. [Online]. Available:

https://agriculture.ec.europa.eu/common-agricultural-policy_en.

[10] S. Zainali, S. Ma Lu, Á. Fernández-Solas, A. Cruz-Escabias, E. F. Fernández, T. E. Khalil Zidane, E. H. Honningdalsnes, M. M. Nygård, J. Leloux, M. Berwind, M. Trommsdorff, S. Amaducci, S. Gorjian and P. E. Campana, "Modelling, simulation, and optimisation of agrivoltaic systems: a comprehensive review," *Applied Energy,* vol. 386, p. 125558, 2025.

[11] D. Berrian, G. Chhapia and J. Linder, "Performance of land productivity with single-axis trackers and shade-intolerant crops in agrivoltaic systems," *Applied Energy,* vol. 384, p. 125471, 2025.

[12] D. Mazzeo, A. Di Zio, C. Pesenti and S. Leva, "Optimizing agrivoltaic systems: A comprehensive analysis of design, crop productivity and energy performance in open-field configurations," *Applied Energy,* vol. 390, p. 125750, 2025.

[13] C. Toledo and A. Scognamiglio, "Agrivoltaic Systems Design and Assessment: A Critical Review, and a Descriptive Model towards a Sustainable Landscape Vision (Three-Dimensional Agrivoltaic Patterns)," *Sustainability,* vol. 13, no. 12, p. 6871, 2021.

[14] Fraunhofer Institute for Solar Energy Systems ISE, "Dual yield on arable land: Guideline for agrivoltaics published," 2021.

[15] National Renewable Energy Laboratory (NREL), "U.S. solar photovoltaic system and energy storage cost benchmark: Q1 2021," 2021.

[16] P. Zippenfenig, "Open-Meteo.com Weather API [Computer software]," *Zenodo,* 2023.

[17] Red Eléctrica de España, S.A.U. (REE), "Sistema de Información del Operador del Sistema (e·sios)," [Online]. Available: https://www.esios.ree.es/es#. [Accessed 2025].

[18] J. Calatrava and D. Martínez Granados, "Valoración económica del uso del agua en el regadío del sistema de explotación Vinalopó-Alacantí de la Demacración Hidrográfica del Júcar y análisis del impacto de la sustitución de extracciones subterráneas por recursos provinientes del Trasvase," 2021.

[19] Revista Mercados, "Mercados. Revista del Sector Hortofrutícola," 2022. [Online]. Available: https://revistamercados.com/los-citricultores-cobran-entre-008-012-e-kg. [Accessed 2025].

[20] Food and Agriculture Organization of the United Nations, "Databases & Software - Crop information for citrus," [Online]. Available: https://www.fao.org/land-water/databases-and-software/crop-information/citrus/en/. [Accessed 2025].

[21] S. S. Chandel, M. Nagaraju Naik and R. Chandel, "Review of solar photovoltaic water pumping system technology for irrigation and community drinking water supplies," *Renewable and Sustainable Energy Reviews,* vol. 49, pp. 1084-1099, 2015.

[22] I. Reda and A. Andreas, "Solar Position Algorithm for Solar Radiation Applications," *SolarEnergy,* vol. 76, no. 5, pp. 577-589, 2004.

[23] Organización de las Naciones Unidas para la Agricultura y la Alimentación, Evapotranspiración del cultivo. Guías para la determinación de los requerimientos de agua de los cultivos, 2006.

[24] HOMER Energy, "How HOMER Calculates the PV Array Power Output," HOMER Energy, [Online]. Available: https://homerenergy.com/products/pro/docs/latest/how_homer_calculates_the_pv_array_power_output.html.

[25] D. L. King, E. E. Boyson and J. A. Kratochvil, "Photovoltaic Array Performance Model," Sandia National Laboratories, Albuquerque, New Mexico, 2004.

[26] European Commission, "Photovoltaic Geographical Information System (PVGIS)," [Online]. Available: https://re.jrc.ec.europa.eu/pvg_tools/es/.

[27] D. Faiman, "Assessing the outdoor operating temperature of photovoltaic modules," *Progress in Photovoltaics,* vol. 16, no. 4, pp. 307-315, 2008.

[28] T. R. Oke, Boundary Layer Climates, 2nd ed., 1987.

[29] J. Howell, M. P. Mengüç and R. Siegel, Thermal radiation heat transfer, sixth edition, 2015.

[30] R. G. Allen, I. A. Walter, R. L. Elliott, T. A. Howell, D. Itenfisu, M. E. Jensen and R. L. Snyder, The ASCE Standardized Reference Evapotranspiration Equation, Reston, VA: American Society of Civil Engineers, 2005.

[31] T. Foster, N. Brozović, A. P. Butler, C. U. Neale, D. Raes, P. Steduto, E. Fereres and T. C. Hsiao, "AquaCrop-OS: An open source version of FAO's crop water productivity model," *Agricultural Water Management,* vol. 181, pp. 18-22, 2017.

[32] German Institute for standardization, *DIN SPEC 91434: Agri-photovoltaic systems - Requirements for primary agricultural use,* 2022.

[33] T. A. Howell, D. W. Meek and J. L. Hatfield, "Relationship of photosynthetically active radiation to shortwave radiation in the San Joaquin Valley," *Agricultural Meteorology,* vol. 28, no. 2, pp. 157-175, 1983.

[34] X.-G. Zhu, S. P. Long and D. R. Ort, "Improving Photosynthetic Efficiency for Greater Yield," *Annual Review of Plant Biology,* vol. 61, pp. 235-261, 2010.

[35] B. Liu, L. Liu, S. Asseng, X. Zou, J. Li, W. Cao and Y. Zhu, "Modelling the effects of heat stress on post-heading durations in wheat: A comparison of temperature response routines," *Agricultural and Forest Meteorology,* vol. 222, pp. 45-58, 2016.

[36] J. L. Monteith, "Climate and the efficiency of crop production in Britain," *Philos Trans R Soc Lond B Biol Sci,* vol. 281, no. 980, pp. 277-294, 1977.